EUROPEAN ORGANIZATION FOR NUCLEAR RESEARCH

CERN-EP/83-73
3 June 1983

EXPERIMENTAL OBSERVATION OF LEPTON PAIRS OF INVARIANT MASS AROUND 95 GeV/c^2 AT THE CERN SPS COLLIDER

UA1 Collaboration, CERN, Geneva, Switzerland

Aachen[1]-Annecy (LAPP)[2]-Birmingham[3]-CERN[4]-Helsinki[5]-Queen Mary College, London[6]-Paris (Coll. de France)[7]-Riverside[8]-Rome[9]-Rutherford Appleton Lab.[10]-Saclay (CEN)[11]-Vienna[12] Collaboration

G. Arnison[10], A. Astbury[10], B. Aubert[2], C. Bacci[9], G. Bauer**, A. Bézaguet[4], R. Böck[4], T.J.V. Bowcock[6], M. Calvetti[4], P. Catz[2], P. Cennini[4], S. Centro[4], F. Ceradini[4,9], S. Cittolin[4], D. Cline**, C. Cochet[11], J. Colas[2], M. Corden[3], D. Dallman[4,12], D. Dau***, M. DeBeer[11], M. Della Negra[2,4], M. Demoulin[4], D. Denegri[11], A. Di Ciaccio[9], D. DiBitonto[4], L. Dobrzynski[7], J.D. Dowell[3], K. Eggert[1], E. Eisenhandler[6], N. Ellis[4], P. Erhard[1], H. Faissner[1], M. Fincke***, G. Fontaine[7], R. Frey[8], R. Frühwirth[12], J. Garvey[3], S. Geer[7], C. Ghesquière[7], P. Ghez[2], W.R. Gibson[6], Y. Giraud-Héraud[7], A. Givernaud[11], A. Gonidec[2], G. Grayer[10], T. Hansl-Kozanecka[1], W.J. Haynes[10], L.O. Hertzberger*, C. Hodges[8], D. Hoffmann[1], H. Hoffmann[4], D.J. Holthuizen*, R.J. Homer[3], A. Honma[6], W. Jank[4], G. Jorat[4], P.I.P. Kalmus[6], V. Karimäki[5], R. Keeler[6], I. Kenyon[3], A. Kernan[8], R. Kinnunen[5], W. Kozanecki[8], D. Kryn[4,7], F. Lacava[9], J.-P. Laugier[11], J.-P. Lees[2], H. Lehmann[1], R. Leuchs[1], A. Lévêque[11,4], D. Linglin[2], E. Locci[11], J.-J. Malosse[11], T. Markiewicz[4], G. Maurin[4], T. McMahon[3], J.-P. Mendiburu[7], M.-N. Minard[2], M. Mohammadi**, M. Moricca[9], K. Morgan[8], H. Muirhead+, F. Muller[4], A.K. Nandi[10], L. Naumann[4], A. Norton[4], A. Orkin-Lecourtois[7], L. Paoluzi[9], F. Pauss[4], G. Piano Mortari[9], E. Pietarinen[5], M. Pimiä[5], A. Placci[4], J.P. Porte[4], E. Radermacher[1], J. Ransdell[8], H. Reithler[1], J.-P. Revol[4], J. Rich[11], M. Rijssenbeek[4], C. Roberts[10], J. Rohlf[4], P. Rossi[4], C. Rubbia[4], B. Sadoulet[4], G. Sajot[7], G. Salvi[6], G. Salvini[9], J. Sass[11], J. Saudraix[11], A. Savoy-Navarro[11], D. Schinzel[4], W. Scott[10], T.P. Shah[10], M. Spiro[11], J. Strauss[12], J. Streets[3], K. Sumorok[4], F. Szoncso[12], D. Smith[8], C. Tao*, G. Thompson[6], J. Timmer[4], E. Tscheslog[1], J. Tuominiemi[5], B. Van Eijk*, J.-P. Vialle[4], J. Vrana[7], V. Vuillemin[4], H.D. Wahl[12], P. Watkins[3], J. Wilson[3], C. Wulz[12], G.Y. Xie[4], M. Yvert[2], E. Zurfluh[4]

(Submitted to Physics Letters B)

---

*) NIKHEF, Amsterdam, The Netherlands.
**) University of Wisconsin, Madison, Wisconsin, USA.
***) University of Kiel, Fed. Rep. Germany.
+) Visitor from the University of Liverpool, England.

ABSTRACT

We report the observation of four electron-positron pairs and one muon pair which have the signature of a two-body decay of a particle of mass ~ 95 GeV/c^2. These events fit well the hypothesis that they are produced by the process $\bar{p} + p \rightarrow Z^0 + X$ (with $Z^0 \rightarrow \ell^+ + \ell^-$), where Z^0 is the Intermediate Vector Boson postulated by the electroweak theories as the mediator of weak neutral currents.

1. INTRODUCTION

We have recently reported the observation of large invariant mass electron-neutrino pairs [1] produced in high-energy collisions at the CERN Super Proton Synchrotron (SPS) [2]. The most likely interpretation of these events is that they are the leptonic decays of charged intermediate vector bosons W^+ and W^- mediating ordinary weak interactions.

We have now extended our search to their neutral partner Z^0, responsible for neutral currents. As in our previous work, production of intermediate vector bosons is achieved with proton-antiproton collisions at $\sqrt{s}$ = 540 GeV in the UA1 detector [3], except that now we search for electron and muon pairs rather than for electron-neutrino coincidences. The process is then:

$$\begin{array}{l} \bar{p} + p \rightarrow Z^0 + X \\ \qquad\quad \hookrightarrow e^+ + e^- \quad \text{or} \quad \mu^+ + \mu^- \end{array} \tag{1}$$

The paper is based on an early analysis of a sample of collisions with an integrated luminosity of 55 nb^{-1}. In this event sample, 27 $W^{\pm} \rightarrow e^{\pm}\nu$ events have been recorded [4]. According to minimal SU(2) × U(1), the Z^0 mass is predicted to be [5] $m_{Z^0} = 94 \pm 2.5$ GeV/c^2. The reaction (1) is then approximately a factor of 10 less frequent than the corresponding $W^{\pm}$ leptonic decay channels [6]. A few events of type (1) are therefore expected in our muon or electron samples. Evidence for the existence of the Z^0 in the range of masses accessible to the UA1 experiment can also be drawn from weak-electromagnetic interference experiments at the highest PETRA energies, where deviations from point-like expectations have been reported [7].

This paper deals with four e^+e^- pairs and one $\mu^+\mu^-$ pair, consistent with a common value of invariant mass and with the general expectations for lepton pairs from Z^0 decay.

2. DETECTOR

The UA1 apparatus has already been described [1]. We limit our discussion to those components which are relevant to the identification and measurement of muons and electrons.

The momenta of charged tracks are determined by deflection in the central dipole magnet generating a field of 0.7 T over a volume of $7 \times 3.5 \times 3.5$ m^3. Tracks are recorded by the central detector (CD) [8], a cylindrical volume of drift chambers 5.8 m in length and 2.3 m in diameter, surrounding the beam crossing region. Accuracy for high-momentum tracks is dominated by the localization error of the electrons drifting in the gas; it is about 100 μm close to the anode wires and 350 μm after 22 cm, the longest drift path. At this stage we find no evidence of significant additional systematic errors, even for the highest momentum tracks [9]. Ionization can be measured to an accuracy of about ±10% for a 1 m long track. This allows identification of narrow, high-energy particle bundles (e^+e^- pairs), even if they cannot be resolved by the digitizings.

The large-angle section of electromagnetic and hadronic calorimetry [1] extends to angles of about 5° with respect to the beam pipe, and it consists of lead/scintillator stacks followed by the instrumented iron of the magnet yoke used as a hadron calorimeter. Additional calorimetry [1], both electromagnetic and hadronic, extends to forward regions, down to 0.2°. Electrons of the present sample have been recorded by the central section of the e.m. calorimetry, consisting of 48 semicylindrical lead/scintillator modules, with an inner radius of 1.36 m, arranged in two cylindrical half-shells, one on either side of the beam axis. Each module (gondola) extends over approximately 180° in azimuth and measures 22.5 cm in the beam direction. Light produced in each of the four separate segmentations in depth (3.3/6.6/9.9/6.6 X_0) is seen by wavelength shifter plates on each side of the stack, which are in turn connected to four photomultipliers (PMs), two at the top and two at the bottom. Light attenuation is exploited in order to further improve the calorimeter information for localized energy

depositions: top and bottom PMs give the azimuthal angle ϕ with error $\Delta\phi$ (rad) = $= 0.3/\sqrt{E\ (GeV)}$. Likewise, localization of the coordinate x (along the beam direction) is determined, using the appropriate PMs pairings, to an accuracy Δx (cm) = $= 6.3/\sqrt{E\ (GeV)}$ for normal incident tracks. Very inclined tracks have a substantially worse localization. Energy resolution, using all four segments and PMs, is $\Delta E/E = 0.15/\sqrt{E\ (GeV)}$. The properties of these detectors were extensively investigated in test beams. Energy calibrations are performed periodically with a strong, collimated ^{60}Co source and detailed scans over the whole detector surface.

High-energy particles are identified by their behaviour as they traverse the calorimeters. Isolated electrons are identified by their characteristic transition curve, and in particular by the lack of penetration in the hadron calorimeter behind them. The performance of the detectors with respect to hadrons and electrons has been studied extensively in a test beam as a function of the energy, the angle of incidence, and the position of impact. The fraction of hadrons (pions) delivering an energy deposition E_c below a given threshold in the hadron calorimeter is a rapidly falling function of energy, amounting to about 0.3% for $p \simeq$ $\simeq$ 40 GeV/c and $E_c < 200$ MeV. Under these conditions, 98% of electrons are detected.

Isolated muons traverse the calorimeters and the added absorbers without deviations beyond those of multiple scattering and without significant energy deposition in excess of ionization losses in the four e.m. calorimeter and two hadron calorimeter segments. In order to detect muon tracks, 50 large drift chambers [10], nearly 4 m × 6 m in size, surround the whole detector, covering a very large area of $\sim$ 500 m^2. Each chamber consists of two orthogonal layers of drift tubes with two planes per projection. We have chosen a staggered arrangement for adjacent planes, thus resolving the left-right ambiguity and at the same time compensating for the inefficiency from the dead spaces between tubes. The extruded aluminium drift tubes have a cross-section of 45 mm × 150 mm, leading to a maximum drift length of 70 mm. An average spatial resolution of 300 μm has been achieved throughout the sensitive volume of the tubes. In order to reach a good

angular resolution of the muon tracks, a second set of four planes is placed 60 cm away from the first one. This long lever arm was chosen in order to reach an angular resolution of few milliradians, comparable to the multiple scattering angle of high-energy muons, typically 3 mrad at 40 GeV/c.

An independent momentum determination of muons traversing the magnetized iron yoke is performed using the known position of the interaction vertex and the track coordinates after the iron. With an appropriate algorithm which reduces effects of multiple scattering [11], excellent agreement is found between momentum measurements in the central detector and the magnetized iron for vertical cosmic-ray muons in the momentum range 10 to 50 GeV/c. The relative precision of the momentum measurement within the iron is found to be $\Delta p/p \simeq 0.20$, in agreement with expectations, mainly due to multiple scattering. Cosmic-ray muons were also used to verify the relative alignments of the central and muon detectors.

The calorimeters have been made completely hermetic down to angles of 0.2° with respect to the direction of the beams. About 97% of the mass of the magnet is calorimetrized. Adding the energy depositions vectorially over the whole solid angle [1], and adding muons, under ideal conditions and with no neutrino emission, one should observe $\Delta\vec{E} = 0$. In practice [1] transverse energy components exhibit small Gaussian residuals centred on zero with r.m.s. deviations well described by the formula $\Delta E_{y,z} = 0.4\cdot\sqrt{\Sigma_i |E_T^i|}$, where all units are in GeV. The longitudinal component ΔE_x is of little use, since it is strongly affected by energy flow escaping undetected through the beam pipes.

3. EVENT SELECTION AND DATA ANALYSIS

The present work is based on a four-week period of data-taking during the months of April and May 1983. The integrated luminosity after subtraction of dead-time and other instrumental inefficiencies was 55 nb^{-1}. As in our previous work [1], four types of trigger were operated simultaneously:

i) An "electron trigger", namely at least 10 GeV of transverse energy deposited in two adjacent elements of the electromagnetic calorimeters covering angles larger than 5° with respect to the beam pipes.

ii) A "muon trigger", namely at least one penetrating track detected in the muon chambers with pseudorapidity $|\eta| \leq 1.3$ and pointing in both projections to the interaction vertex within a specified cone of aperture ±150 mrad. This is accomplished by a dedicated set of hardware processors filtering the patterns of the muon tube hits.

iii) A "jet trigger", namely at least 20 GeV of transverse energy in a localized calorimeter cluster [12].

iv) A global "E_T trigger", with > 50 GeV of total transverse energy from all calorimeters with $|\eta| < 1.4$.

Events for the present paper were further selected by the so-called "express line", consisting of a set of four 168E computers [13] operated independently in real time during the data-taking. A subsample of events with $E_T \geq 12$ GeV in the electromagnetic calorimeters and dimuons are selected and written on a dedicated magnetic tape. These events have been fully processed off-line and further subdivided into four main classes: i) single, isolated electromagnetic clusters with $E_T > 15$ GeV and missing energy events with $E_{miss} > 15$ GeV, in order to extract $W^{\pm} \to e^{\pm}\nu$ events [1,4]; ii) two or more isolated electromagnetic clusters with $E_T >$ > 25 GeV for $Z^0 \to e^+e^-$ candidates; iii) muon pair selection to find $Z^0 \to \mu^+\mu^-$ events; and iv) events with a track reconstructed in the central detector, of transverse momentum within one standard deviation, $p_T \geq 25$ GeV/c, in order to evaluate some of the background contributions. We will discuss these different categories in more detail.

4. EVENTS WITH TWO ISOLATED ELECTRON SIGNATURES

An electron signature is defined as a localized energy deposition in two contiguous cells of the electromagnetic detectors with $E_T > 25$ GeV, and a small (or no) energy deposition ($\leq$ 800 MeV) in the hadron calorimeters immediately behind them. The isolation requirement is defined as the absence of charged tracks with momenta adding up to more than 3 GeV/c of transverse momentum and pointing towards the electron cluster cells. The effects of the successive cuts on the invariant electron-electron mass are shown in fig. 1. Four e^+e^- events survive cuts,

consistent with a common value of (e^+e^-) invariant mass. They have been carefully studied using the interactive event display facility MEGATEK. One of these events is shown in figs. 2a and 2b. The main parameters of the four events are listed in tables 1 and 3. As one can see from the energy deposition plots (fig. 3), their dominant feature is of two very prominent electromagnetic energy depositions. All events appear to balance the visible total transverse energy components; namely, there is no evidence for the emission of energetic neutrinos. Except for one track of event D which travels at less than 15° parallel to the magnetic field, all tracks are shown in fig. 4a, where the momenta measured in the central detector are compared with the energy deposition in the electromagnetic calorimeters. All tracks but one have consistent energy and momentum measurements. The low-momentum track of event C is interpreted as being due to a hard bremsstrahlung process, either internal or in the corrugated vacuum chamber and detector walls. We have estimated the probability that one of the electrons in the sample radiates at least 70% of its energy and found it to be $\sim 1/4$ [14], assuming that the "average" thickness is traversed by all the tracks. Furthermore, sensitive checks of the correctness of the electron assignment for the tracks can be obtained by comparing the impact of the electron tracks on the e.m. calorimeters as measured by the central detector with the centroid of the energy deposition measured from the ratio of PM signals. This test is particularly sensitive along the x-direction (see fig. 4b) and it appears to be entirely consistent with expectations based on the electron charge assignments of the two tracks. The average invariant mass of the pairs, combining the four consistent values, is (95.2 ± 2.5) GeV/c^2 (table 3).

5. EVENTS WITH TWO MUON TRACKS

Events from the dimuon trigger flag have been submitted to the additional requirement that there is at least one muon track reconstructed off line in the muon chambers, and with one track in the central detector of reasonable projected length ($\geq$ 40 cm) and $p_T \geq 7$ GeV/c. Only 42 events survive these selection criteria. Careful scanning of these events has led to only one clean dimuon event, with two

"isolated" tracks (fig. 5). Most of the events are due to cosmics. Parameters are given in tables 2 and 3. Energy losses in the calorimeters traversed by the two muon tracks are well within expectations of ionization losses of high-energy muons (fig. 6a). The position in the coordinate and the angles at the exit of the iron absorber (fig. 6b) are in agreement with the extrapolated track from the central detector, once multiple scattering and other instrumental effects have been calibrated with $p > 50$ GeV cosmic-ray muons traversing the same area of the apparatus. There are two ways of measuring momenta, either in the central detector or using the muon detector. Both measurements give consistent results. Furthermore, if no neutrino is emitted (as suggested by the electron events which exhibit no missing energy), the recoil of the hadronic debris, which is significant for this event, must be equal to the transverse momentum of the $(\mu^+\mu^-)$ pair by momentum conservation. The directions of the two muons then suffice to calculate the momenta of the two tracks. Uncertainties of muon parameters are then dominated by the errors of calorimetry. As shown in table 2, this determination is in agreement with magnetic deflection measurements. The invariant mass of the $(\mu^+\mu^-)$ pair is found to be $m_{\mu\mu} = 95.5 \pm 7.3)$ GeV/c^2, in excellent agreement with that of the four electron pairs (see table 3).

6. BACKGROUND ESTIMATES

The most striking feature of the events is their common value of the invariant mass (fig. 7); values agree within a few percent and with expectations from experimental resolution. Detection efficiency is determined by the energy thresholds in the track selection, 15 GeV/c for $e^{\pm}$ and 7 GeV/c for $\mu^{\pm}$. Most "trivial" sources of background are not expected to exhibit such a clustering at high masses. Also, most backgrounds would have an equal probability for $(e\mu)$ pairs, which are not observed. Nevertheless, we have considered several possible spurious sources of events:

i) Ordinary large transverse momentum jets which fragment into two apparently isolated, high-momentum tracks, both simulating either muons or electrons. To evaluate this effect, events with (hadronic) tracks of momenta compatible with $p_T > 25$ GeV/c were also selected in the express line. After requiring that the track is isolated, one finds one surviving event with transverse energy $\simeq 25$ GeV in a sample corresponding to 30 nb^{-1}. Including the probability that this track simulates either a muon ($\sim 2 \times 10^{-3}$) or an electron ($\sim 6 \times 10^{-3}$), we conclude that this effect is negligible [15]. Note that two tracks (rather than one) are needed to simulate our events (probabilities must be squared!) and that the invariant mass of the events is much higher than the background. The background is expected to fall approximately like m^{-5} according to the observed jet-jet mass distributions [16].

ii) Heavy-flavoured jets with subsequent decay into leading muons or electrons. In the 1982 event sample (11 nb^{-1}), two events have been observed with a single isolated muon of $p_T > 15$ GeV and one electron event with $p_T > 25$ GeV/c. Some jet activity in the opposite hemisphere is required. One event exhibits also a significant missing energy. Once this is taken into account they all have a total (jet+jet+lepton+neutrino) transverse mass of around 80 GeV/c^2, which indicates that they are most likely due to heavy-flavour decay of W particles. This background will be kinematically suppressed at the mass of our five events. Nevertheless, if the fragmentation of the other jet is also required to give a leading lepton and no other visible debris, this background contributes at most to 10^{-4} events. Monte Carlo calculations using ISAJET lead to essentially the same conclusion [6].

iii) Drell-Yan continuum. The estimated number and the invariant mass distribution make it negligible [17].

iv) W^+W^- pair production is expected to be entirely negligible at our energy [18].

v) Onium decay from a new quark, of mass compatible with the observation (~ 95 GeV/c^2). Cross-sections for this process have been estimated by different authors [19], and they appear much too small to account for the desired effect.

In conclusion, none of the effects listed above can produce either the number or the features of the observed events.

7. DILEPTON EVENTS AS Z^0 LEPTONIC DECAYS

All the observations are in agreement with the hypothesis that events are due to the production and decay of the neutral intermediate vector boson Z^0 according to reaction (1). The transverse momentum distribution is shown in fig. 7, compared with the observed distributions for the $W^{\pm} \to e\nu$ events [4] and with QCD calculations [20]. The muon event and one of the electron events (event B) have visible jet structure. Other events are instead apparently structureless.

From our observation, we deduce a mass value for the Z^0 particle,

$$m_{Z^0} = (95.2 \pm 2.5) \text{ GeV}/c^2 .$$

The half width based on the four electron events is 3.1 GeV/c^2 (< 5.1 GeV/c^2 at 90% c.l.), consistent with expectation from the experimental resolution and the natural Z^0 width [5], $\Gamma_{Z^0} = 3.0$ GeV. At this point it is important to stress that the final calibration of the electromagnetic calorimeters is still in progress and that small scale shifts are still possible, most likely affecting *both* the $W^{\pm}$ and Z^0 mass values. No e.m. radiative corrections have been applied to the masses [14].

We now compare our result with the prediction of standard SU(2) × U(1). Employing the renormalized weak mixing angle $\sin^2 \theta_w (m_W)$ defined by modified minimal subtraction, we find to $O(\alpha)$:

$$\sin^2 \theta_w (m_W) = \left(\frac{38.5 \text{ GeV}}{m_W}\right)^2 .$$

From our preliminary result [4] we find

$$\sin^2 \theta_w (m_W) = (0.226 \pm 0.011) ,$$

in excellent agreement with the extrapolation from the world low-energy data [5] $\sin^2 \theta_w (m_W) = (0.236 \pm 0.030)$. If we then parametrize the Z^0 mass with the well-known formula $m_{Z^0}^2 = m_W^2/\rho \cos^2 \theta_w (m_W)$, we find $\rho = (0.94 \pm 0.06)$ (see fig. 9),

in excellent agreement with the prediction of the minimal model, where one usually assumes that $\rho = 1$. Potential deviations from this value could come from higher Higgs representations, additional fermion generations, dynamical symmetry effects, etc. Within the accuracy of our result, none of these effects needs to be invoked.

Acknowledgements

The continued success of the collider and the steady increase in luminosity which have made this result possible, depend critically upon the superlative performance of the whole CERN accelerator complex, which was magnificently operated by its staff. We thank W. Kienzle who, as coordinator, balanced very effectively the sometimes conflicting interests of the physicists and accelerator staff. We have received enthusiastic support from the Director General, H. Schopper, and his Directorate, for the results emerging from the SPS Collider programme.

We are thankful to the management and staff of CERN and of all participating Institutes who have vigorously supported the experiment.

The following funding Agencies have contributed to this programme:

Fonds zur Förderung der Wissenschaftlichen Forschung, Austria.

Valtion luonnontieteellinen toimikunta, Finland.

Institut National de Physique Nucléaire et de Physique des Particules and Institut de Recherche Fondamentale (CEA), France.

Bundesministerium für Forschung und Technologie, Germany.

Istituto Nazionale di Fisica Nucleare, Italy.

Science and Engineering Research Council, United Kingdom.

Department of Energy, USA.

Thanks are also due to the following people who have worked with the collaboration in the preparation and data collection on the runs described here:

O.C. Allkofer, F. Bernasconi, F. Cataneo, R. Del Fabbro, L. Dumps, D. Gregel, G. Stefanini and R. Wilson.

The whole UA1 Collaboration is very grateful for the unfailing help and friendly advice of Mme Mirella Keller.

REFERENCES AND FOOTNOTES

[1] G. Arnison et al. (UA1 Collaboration), Phys. Lett. 122B (1983) 103.
See also the corresponding result by the UA2 Collaboration: G. Banner et al., Phys. Lett. 122B (1983) 476.

[2] The staff of CERN proton-antiproton project, Phys. Lett. 107B (1981) 306.
C. Rubbia, P. McIntyre and D. Cline, Proc. Int. Neutrino Conference, Aachen, 1976 (Vieweg, Braunschweig, 1977), p. 683.
Study Group, Design study of a proton-antiproton colliding beam facility, CERN/PS/AA 78-3 (1978), reprinted in Proc. Workshop on Producing High-Luminosity, High-Energy Proton-Antiproton Collisions, Berkeley, 1978 (report LBL-7574, UC34c), p. 189.

[3] UA1 proposal: A 4π solid-angle detector for the SPS used as a proton-antiproton collider at a centre-of-mass energy of 540 GeV, CERN/SPSC 78-06 (1978).
M. Barranco Luque et al., Nucl. Instrum. Methods 176 (1980) 175.
M. Calvetti et al., Nucl. Instrum. Methods 176 (1980) 255.
K. Eggert et al., Nucl. Instrum. Methods 176 (1980) 217 and 223.
A. Astbury et al., Phys. Scr. 23 (1981) 397.

[4] G. Arnison et al. (UA1 Collaboration), in preparation. Since the run is at present continuing at the CERN SPS Collider, the paper is likely to contain an event sample significantly larger than what is reported here. The result for the mass of the W is $m_W = (81 \pm 2)$ GeV/c^2.

[5] S. Weinberg, Phys. Rev. Lett. 19 (1967) 1264.
A. Salam, Proc. 8th Nobel Symposium, Aspenäsgården, 1968 (Almqvist and Wiksell, Stockholm, 1968), p. 367.
S.L. Glashow, Nuclear Phys. 22 (1961) 579.
For latest parameters see W.J. Marciano and Z. Parsa, Proc. AIP Dept. of Particles and Fields Summer Study on Elementary Particle Physics and Future Facilities, Snowmass, Colorado, 1982 (AIP, New York, 1983), p. 155.

The values used in this paper come from J. Kim et al., Rev. Mod. Phys. 53 (1981) 211, and from I. Liede and M. Roos, Nucl. Phys. B167 (1980) 397. The two-parameter fit to ν_μ and $\bar{\nu}_\mu$ data yields $\rho = 1.02 \pm 0.026$ and $\sin^2 \theta_w (m_W) = 0.236 \pm 0.030$ at the W mass. The values for the W and Z masses are then $m_W = 79.3 \, ^{+5.5}_{-4.7}$ GeV/c^2 and $m_Z = 89.9 \pm 4.4$ GeV/c^2. Imposing $\rho = 0.99$ (theoretical) gives $m_W = 83.0 \, ^{+3.0}_{-2.8}$ GeV/c^2 and $m_Z = 93.8 \, ^{+2.5}_{-2.4}$ GeV/c.

[6] F.E. Paige and S.D. Protopopescu, ISAJET program, BNL 29777 (1981). All cross-sections are calculated in the leading log approximation, assuming $SU(2) \times U(1)$.

[7] For a summary of the results of the CELLO, JADE, MARK J and TASSO Collaborations, see M. Davier, Proc. 21st Int. Conf. on High-Energy Physics, Paris, 1982 [J. Phys. (France), No. 12, t. 43 (1982)], p. C3-471. The result quoted is $m_Z = 76 \, ^{+21}_{-11}$ GeV/c^2, or a 2 st. dev. effect from $m_Z = \infty$.

[8] M. Calvetti et al., IEEE Trans. Nucl. Sci. NS-30 (1983) 71.

M. Barranco-Luque et al., Nucl. Instrum. Methods 176 (1980) 175.

M. Calvetti et al., The UA1 central detector, Proc. Int. Conf. on Instrumentation for Colliding Beam Physics, SLAC, Stanford, 1982 (SLAC-250, Stanford, 1982), p. 16.

The UA1 Collaboration, The UA1 data acquisition system, Proc. Int. Conf. on Instrumentation for Colliding Beam Physics, SLAC, Stanford, 1982 (SLAC-250, Stanford, 1982), p. 151.

[9] A large number of cosmic-ray muons traversing both the upper and the lower elements of the central detector were studied, comparing momenta determinations. Events were recorded continuously during the run and within the beam crossing gate (50 ns). Additional data were collected with beams off. This was done in order to ensure the absence of positive ion distortions in the tracks. Apart from the over-all timing, which is fitted from the track as long as there is at least one drift volume crossing, all other calibration constants are identical to those used for actual events.

No evidence for systematic effects, beyond statistical contributions from individual drift distance measurements, are needed to account for momentum measurements up to p > 50 GeV/c.

[10] K. Eggert et al., Nucl. Instrum. Methods 176 (1980) 217.

[11] Correlations between multiple scatterings have been removed using the known relationship between angle and displacement: $\langle x_{ms}^2 \rangle = (k')^2 \langle \phi_{ms}^2 \rangle$ and $\langle x\phi_{ms} \rangle = k\langle \phi_{ms}^2 \rangle$. From known properties of materials, $k' = 2.40$, $k = 1.60$ (units: cm, rad). Cosmic-ray data give $k' = 3.0$ for the azimuth and 3.9 for the dip angle.

[12] The jet cluster is defined as in ref. 1, namely six electromagnetic cells and two hadronic cells immediately behind. Energy responses of calorimeters for hadrons and electrons are somewhat different.

[13] J.T. Carroll, S. Cittolin, M. Demoulin, A. Fucci, B. Martin, A. Norton, J.-P. Porte, P. Ross and K.M. Storr, Data Acquisition using the 168E, Paper presented at the Three-Day In-Depth Review on the Impact of Specialized Processors in Elementary Particle Physics, Padua, 1983, in print.

[14] The inner bremsstrahlung has been calculated according to F.A. Berends and R. Keiss, Instituut-Lorentz, Leiden University, On the process $\bar{q}q \to Z \to \to \ell^+\ell^-(\gamma)$ (to be published).

F.A. Berends et al., Nucl. Phys. B202 (1982) 63.

On the same subject, see G. Passarino and M. Veltman, Nucl. Phys. B160 (1979) 151.

M. Greco et al., Nucl. Phys. B171 (1980) 118 [E: B197 (1982) 543].

V.N. Baier et al., Phys. Rep. 78 (1981) 293.

We are grateful to F.A. Berends for his assistance with this difficult subject. We find that the probability that either electron of the $Z \to e^+e^-$ decay emits more than 70% of the initial particle energy into photons is about 2.3%. External radiation has also been calculated. It amounts to about 3.5% for the average thickness traversed (0.1 radiation length traversed by both electrons). However, large fluctuations can occur as

a result of critical angles due to corrugations in the vacuum pipe, especially around 70°. The faulty track of event C has an angle of emission close to this value.

[15] Electron-pion discrimination has been measured in a test beam in the full energy range and angles of interest. The muon tracks have the following probabilities: i) no interaction: 2×10^{-5} (4×10^{-5}); ii) interaction but undetected by the calorimeter and geometrical cuts: 10^{-4} (4×10^{-4}); iii) decay: 10^{-3} (0.7×10^{-3}). Figures within parenthesis refer to negative tracks.

[16] UA1 Collaboration, Study of jets in $p\bar{p}$ collisions with UA1 calorimetry (presented by J. Sass), and Jet fragmentation at the SPS $p\bar{p}$ Collider (presented by V. Vuillemin), Proc. 18th Rencontre de Moriond, La Plagne, 1983 (Editions Frontières, Dreux, 1983), in preparation.

[17] S.D. Drell and T.M. Yan, Phys. Rev. Lett. 25 (1970) 316.
F. Halzen and D.H. Scott, Phys. Rev. D18 (1978) 3378.
See also ref. 6.
S. Pakvasa, M. Dechantsreiter, F. Halzen and D.M. Scott, Phys. Rev. D20 (1979) 2862.

[18] R. Kinnunen, Proc. Proton-Antiproton Collider Physics Workshop, Madison, 1981 (Univ. Wisconsin, Madison, 1982).
R.W. Brown and K.O. Mikaelian, Phys. Rev. D19 (1979) 922.
R.W. Brown, D. Sahdev and K.O. Mikaelian, Phys. Rev. D20 (1979) 1164.
See also ref. 6.

[19] T.K. Gaisser, F. Halzen and E.A. Paschos, Phys. Rev. D15 (1977) 2572.
R. Baier and R. Rückl, Phys. Lett. 102B (1981) 364.
F. Halzen, Proc. 21st Int. Conf. on High-Energy Physics, Paris, 1982 [J. Phys. (France), No. 12, t. 43 (1982)], p. C3-381.
F.D. Jackson, S. Olsen and S.H.H. Tye, Proc. AIP Dept. of Particles and Fields Summer Study on Elementary Particle Physics and Future Facilities, Snowmass, Colorado, 1982 (AIP, New York, 1983), p. 175.

[20] P. Aurenche and R. Kinnunen, QCD predictions for weak vector boson production in $\bar{p}p$ collisions, in preparation.

P. Aurenche and J. Lindfors, Nucl. Phys. B185 (1981) 274.

P. Chiappetta and M. Greco, Nucl. Phys. B199 (1982) 77, and references quoted therein.

Table 1

Properties of the individual electrons of the pair events

Run, event		Drift chamber measurement						Shower counter measurement					
		p (GeV)	Δp a) (GeV)	Q	dE/dx b)	y c)	φ (deg)	E_{tot} (GeV)	Electromagnetic samples (GeV) S_1	S_2	S_3	S_4	Had. energy H
A	7433 1001	33	$^{+9}_{-6}$	+	1.8 ± 0.3	1.01	144	44	14	27	3	0.0	0.0
		63	$^{+23}_{-13}$	-	1.7 ± 0.2	-1.19	-31	48	6	37	4	0.2	0.0
B	7434 746	27	$^{+19}_{-8}$	+	1.6 ± 0.3	-0.36	131	42	2	18	20	1.3	0.1
		93	$^{+66}_{-28}$	-	1.8 ± 0.2	-1.45	-60	102	42	56	4	0.2	0.0
C	6059 1010	32	$^{+11}_{-6}$	+	1.3 ± 0.2	0.64	67	61	1	37	22	0.6	0.0
		9	$^{+1}_{-1}$	-	1.4 ± 0.1	0.24	-121	48	1	23	23	1.3	0.0
D	7739 1279	d)	d)	d)	d)	-0.19	169	51	1	13	34	2.4	0.0
		50	$^{+50}_{-17}$	-	1.5 ± 0.2	-0.79	-9	55	8	38	9	0.0	0.1

a) ±1σ including systematic errors.
b) Ionization loss normalized to minimum ionizing pion.
c) The rapidity y is defined as positive in the direction of outgoing $\bar{p}$.
d) Unmeasured owing to large dip angle.

Table 2

Properties of the muons of the dimuon event 6600-222

Track parameters					Muon identification				
					Normalized ionization I/I_0		λ_{abs}	μ/CD matching d)	
Q	p (GeV/c)	ℓ (cm)	y	φ (°)	e.m. calorimeter	Hadron calorimeter		Position (cm)	Angle (mrad)
+	$58.8\ ^{+\ 8}_{-\ 6}$ a)								
	60.3 ± 10.8 b)								
	$59.2\ ^{+\ 6.4}_{-\ 5.2}$ c)	170	1.19	-27.6	0.8 ± 0.5	1.2 ± 0.5	10.2	ΔX_1 = -1.3 ± 1.9 ΔX_2 = 11.6 ± 10.7	Δφ = -2 ± 6 ΔΛ = 11 ± 14
-	$63.6\ ^{+\ 30}_{-\ 15}$ a)								
	43.1 ± 6.2 b)								
	$46.1\ ^{+\ 6.1}_{-\ 5.7}$ c)	80	-0.28	119.1	1.2 ± 0.9	1.6 ± 0.8	11.1	ΔX_1 = -0.1 ± 8.0 ΔX_2 = -8.0 ± 8.5	ΔΦ = -6 ± 3 ΔΛ = -9 ± 14

Momentum determination:
a) Central detector and μ chamber (statistical errors only);
b) Transverse momentum balance;
c) Weighted average of (a) and (b);

μ-CD matching:
d) Difference between the extrapolated CD track and the track measured in the μ chambers (see fig. 6).

Remarks:
The acceptance of the single muon trigger starts at a transverse momentum of about 2.5 GeV/c and reaches its full efficiency of 97% at 5.5 GeV/c. The geometrical acceptance of the dimuon trigger, used in this analysis, reduced the acceptance for Z^0 events to about 30%.

Table 3

Mass and energy properties of lepton pair events

Run, event	Lepton pair properties			General event properties			
	Mass [a] (GeV/c^2)	p_T (GeV/c)	x_F [b]	E_{tot} (GeV)	$\Sigma\|E_T\|$ (GeV)	Missing E_T (GeV)	Charged tracks
A 7433 1001	91 ± 5	2.9 ± 0.9	0.02 ± 0.01	274	82	2.1 ± 3.6	27
B 7434 746	97 ± 5	7.9 ± 1.2	0.39 ± 0.01	494	149	9.3 ± 5.0	67
C 6059 1010	98 ± 5	8.0 ± 1.5	0.17 ± 0.01	412	143	3.3 ± 4.8	38
D 7339 1279	95 ± 5	8.4 ± 1.4	0.17 ± 0.01	493	157	0.8 ± 5.0	54
E ($\mu\mu$) 6600 222	95 ± 8	24 ± 5	0.14 ± 0.02	278[c]	128[c]	3.4 ± 5.9[c]	28

a) These errors have been scaled up arbitrarily to 5 GeV to represent the present level of uncertainty in the overall calibration of the e.m. calorimeter which will be recalibrated completely at the end of the present run. This scale factor is not included in the error bars plotted in fig. 8.

b) x_F is defined as the longitudinal momentum of the dilepton divided by beam energy.

c) Includes the muon energies.

Figure captions

Fig. 1 : Invariant mass distribution (uncorrected) of two electromagnetic clusters: a) with $E_T > 25$ GeV; b) as above and a track with $p_T > 7$ GeV/c and projected length > 40 cm pointing to the cluster. In addition, a small energy deposition in the hadron calorimeters immediately behind (< 0.8 GeV) ensures the electron signature. Isolation is required with $\sum p_T < 3$ GeV/c for all other tracks pointing to the cluster. c) The second cluster also has an isolated track.

Fig. 2 : a) Event display. All reconstructed vertex associated tracks and all calorimeter hits are displayed.

b) The same, but thresholds are raised to $p_T > 2$ GeV/c for charged tracks and $E_T > 2$ GeV for calorimeter hits. We remark that only the electron pair survives these mild cuts.

Fig. 3 : Electromagnetic energy depositions at angles > 5° with respect to the beam direction for the four electron pairs.

Fig. 4 : a) Magnetic deflection in 1/p units compared to the inverse of the energy deposited in the electromagnetic calorimeters. Ideally, all electrons should lie on the 1/E = 1/p line.

b) Normalized deviation between the track hit as computed from the central detector and calorimetry centroids. The deviations have been measured in test beam runs, for a) $W \to e\nu$ events and b) $Z^0 \to e^+e^-$ candidates. The continuous line is a unit variance Gaussian.

Fig. 5 : Display for the high-invariant-mass muon pair event: a) without cuts and b) with $p_T > 1$ GeV thresholds for tracks and $E_T > 0.5$ GeV for calorimeter hits.

Fig. 6 : a) Normalized energy losses in calorimeter cells traversed by the two muon tracks.

Fig. 6 : b) Arrows show residuals in angle and position for the muon track. Distributions come from cosmic-ray calibration with $p > 50$ GeV/c.

Fig. 7 : Transverse momentum spectra: a) for $W \to e\nu$ events, and b) $Z^0 \to \ell^+\ell^-$ candidates. The lines represent QCD predictions (ref. 20).

Fig. 8 : Invariant masses of lepton pairs.

Fig. 9 : Mass of charged versus neutral intermediate vector bosons. Values of parameters ρ and $\sin^2 \theta_W$ (m_W) according to SU(2) × U(1) can be associated with our measured point.

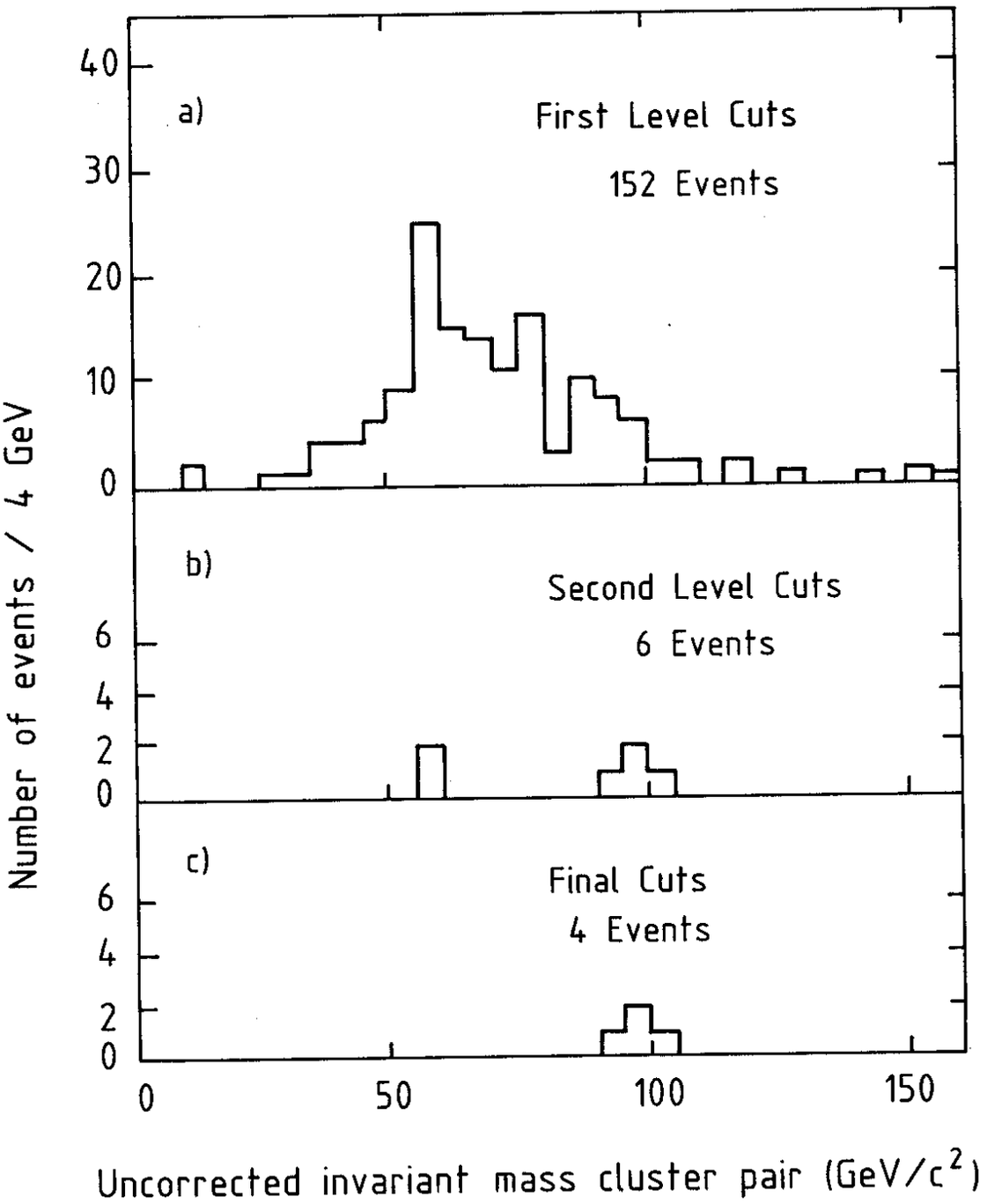
a)
First Level Cuts
152 Events
b)
Second Level Cuts
6 Events
c)
Final Cuts
4 Events
Number of events / 4 GeV
Uncorrected invariant mass cluster pair (GeV/c²)
0
50
100
150
40
30
20
10
6
4
2

Fig. 1

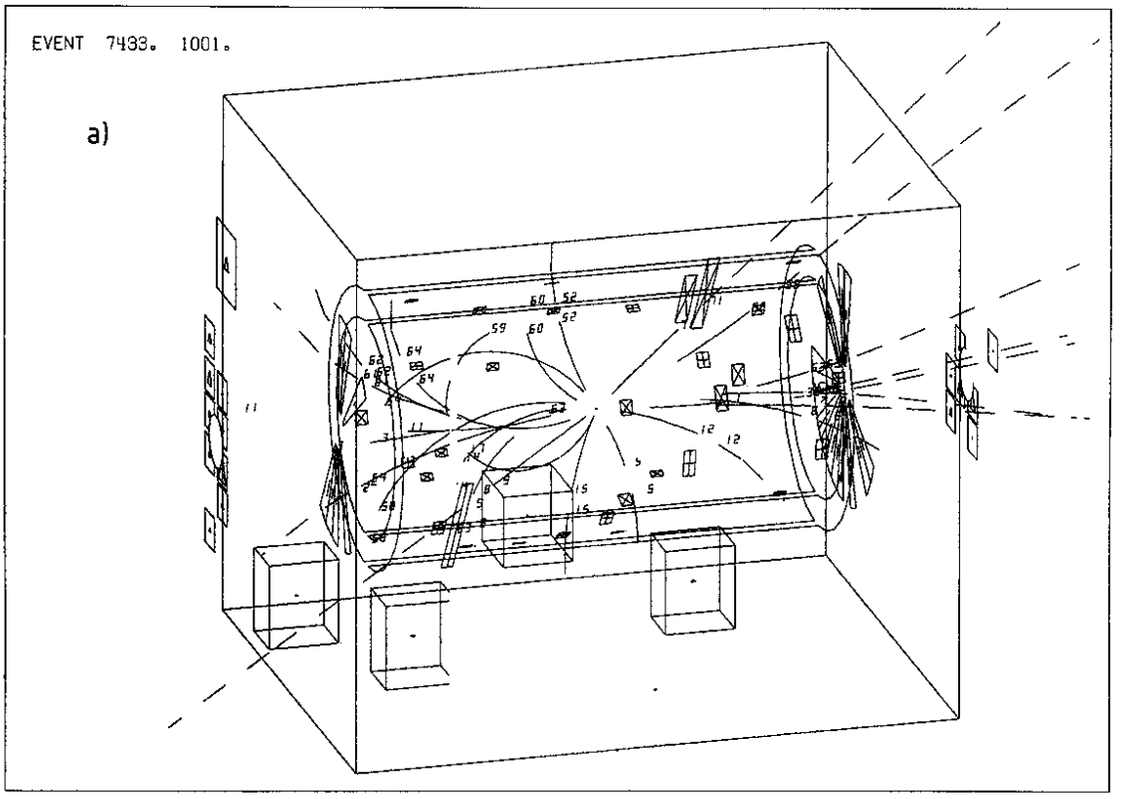

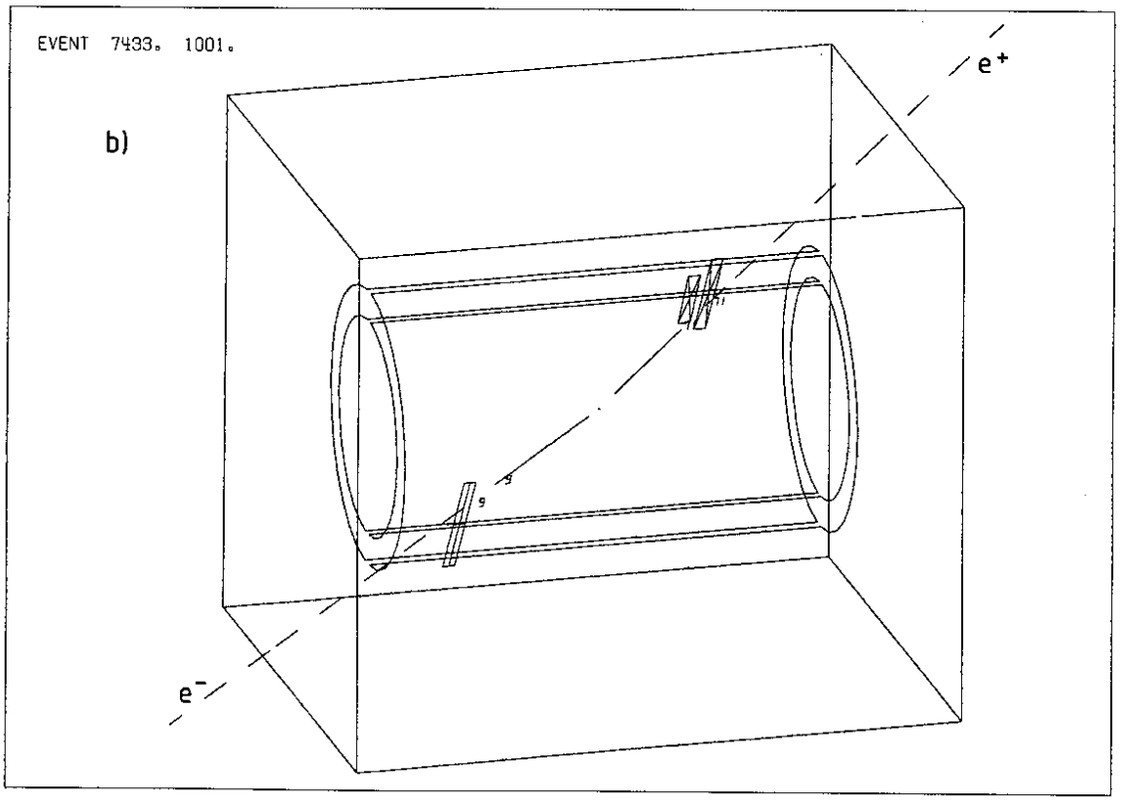

Fig. 2

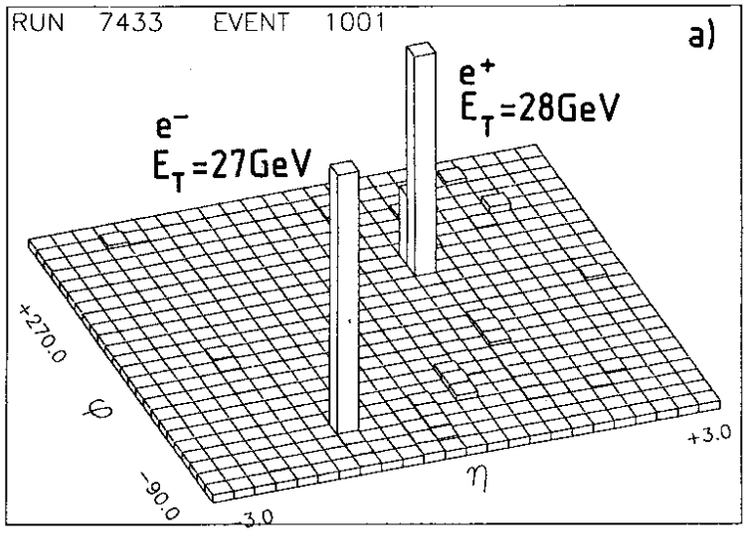
RUN 7433 EVENT 1001
a)
e⁻
E_T=27GeV
e⁺
E_T=28GeV
+270.0
φ
-90.0
-3.0
η
+3.0

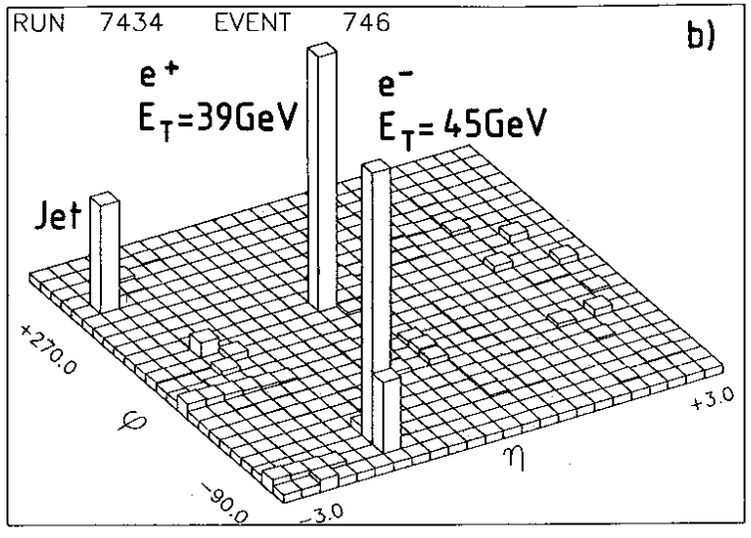
RUN 7434 EVENT 746
b)
e⁺
E_T=39GeV
e⁻
E_T=45GeV
Jet
+270.0
φ
-90.0
-3.0
η
+3.0

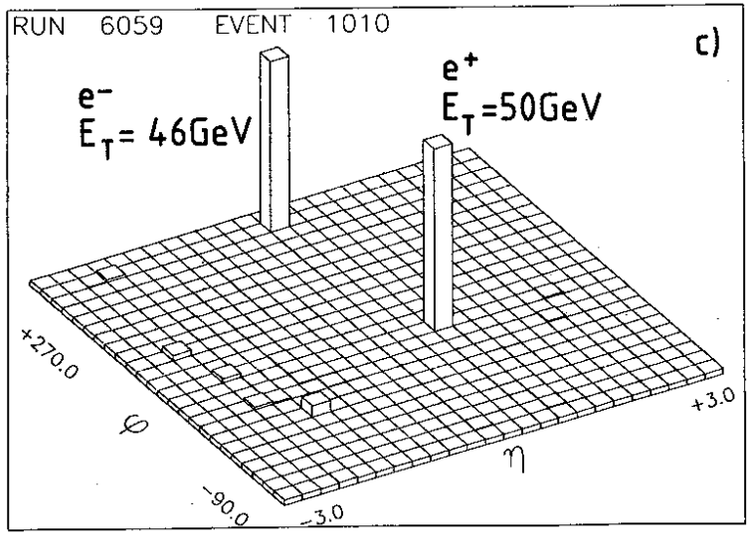
RUN 6059 EVENT 1010
c)
e⁻
E_T=46GeV
e⁺
E_T=50GeV
+270.0
φ
-90.0
-3.0
η
+3.0

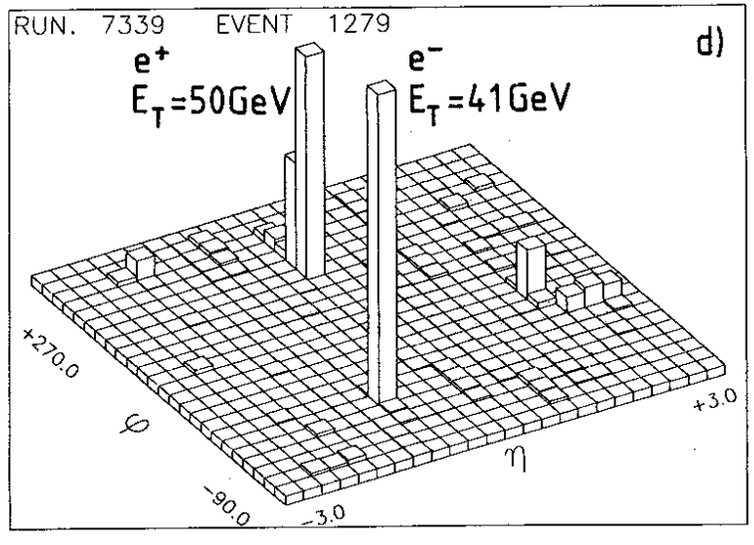
RUN. 7339 EVENT 1279
d)
e⁺
E_T=50GeV
e⁻
E_T=41GeV
+270.0
φ
-90.0
-3.0
η
+3.0

Fig. 3

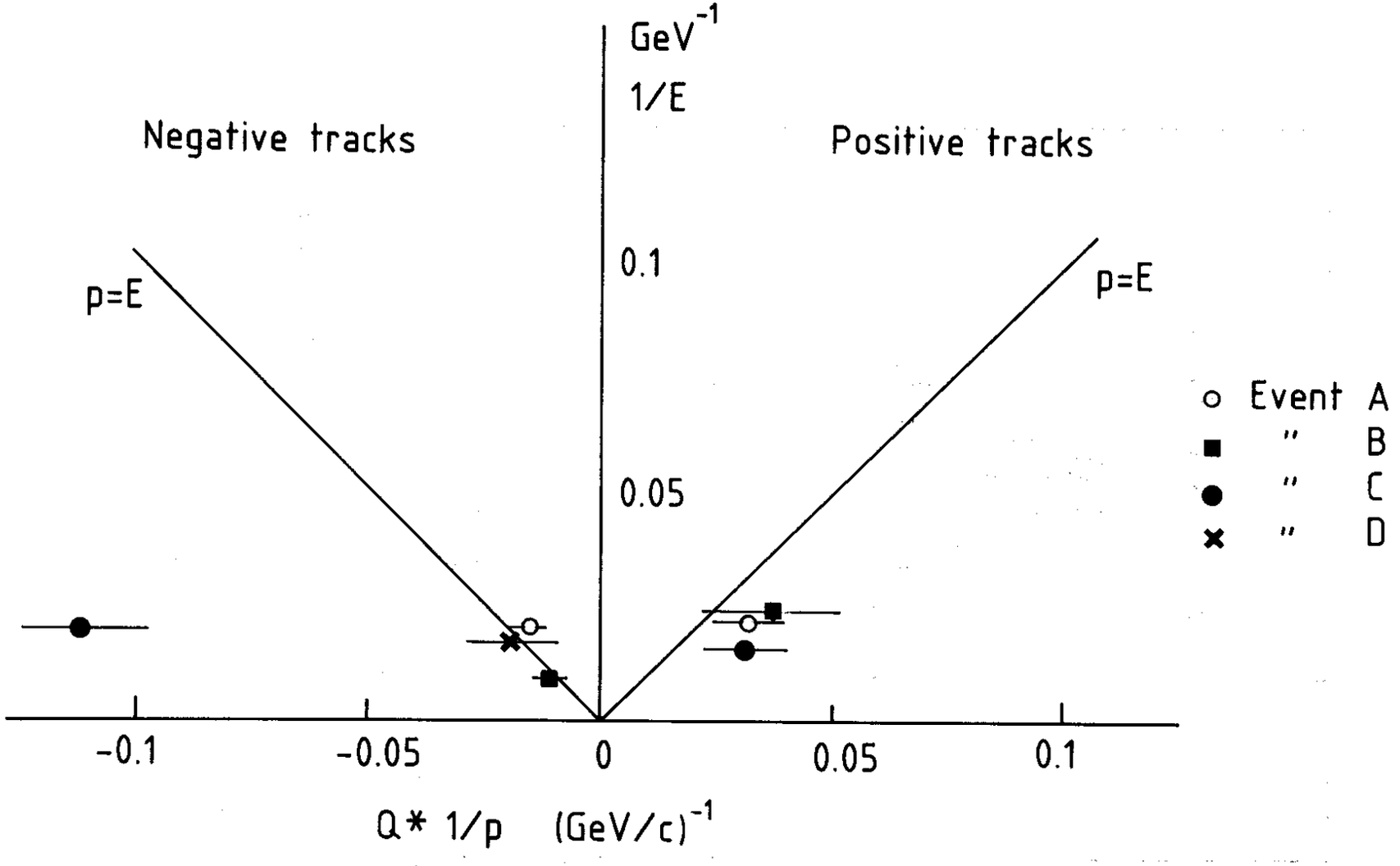
GeV^{-1}
1/E
Negative tracks
Positive tracks
p=E
p=E
0.1
0.05
-0.1
-0.05
0
0.05
0.1
Q* 1/p (GeV/c)$^{-1}$
Event A
" B
" C
" D

Fig. 4a

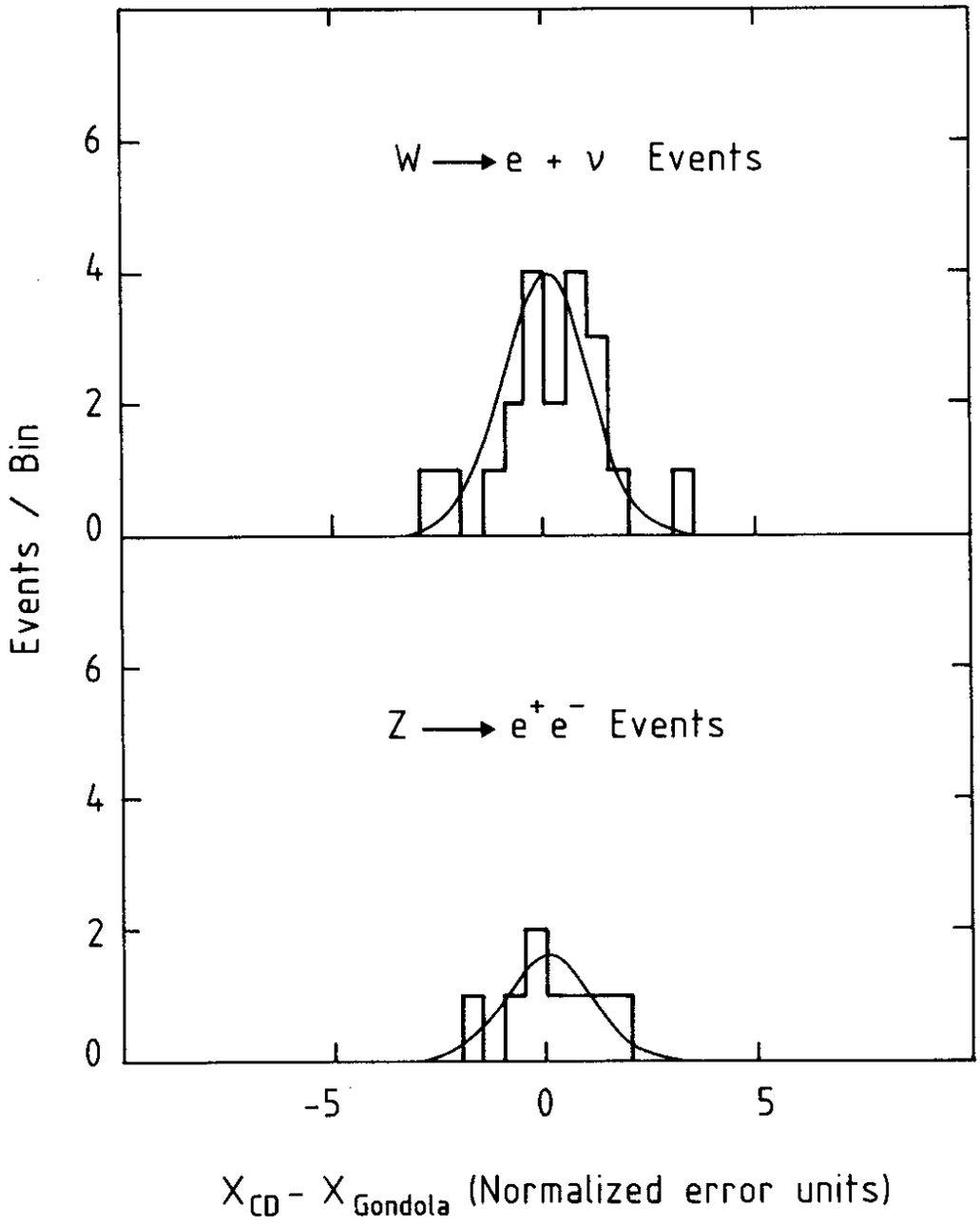
W ⟶ e + ν Events
Z ⟶ e⁺e⁻ Events
Events / Bin
6
4
2
0
-5
0
5
X_CD - X_Gondola (Normalized error units)

Fig. 4b

EVENT 6600. 222.

a)

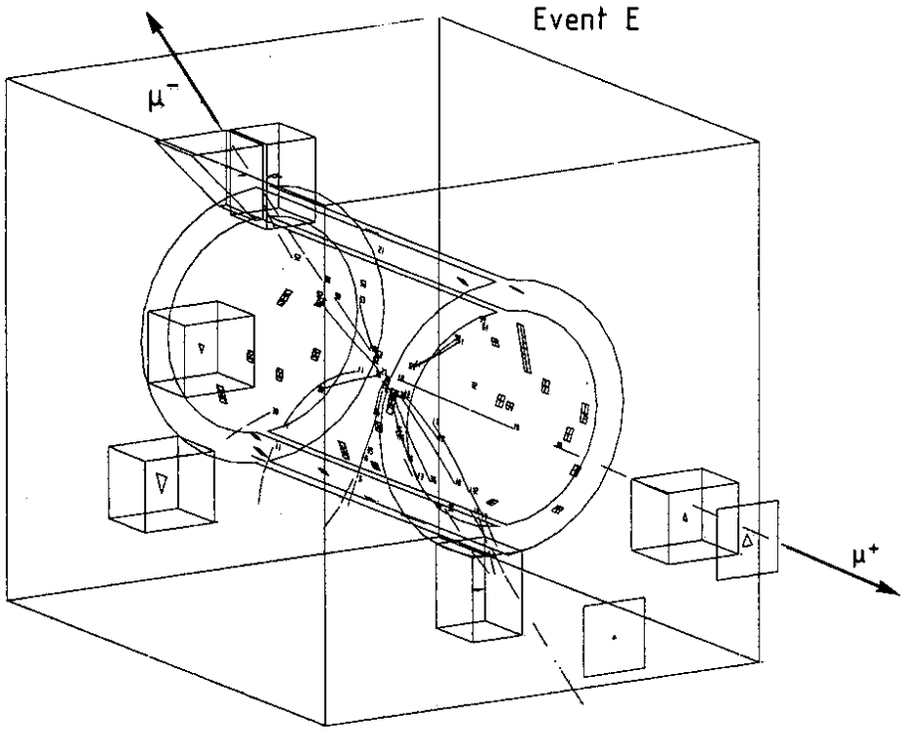

EVENT 6600. 222.

b)

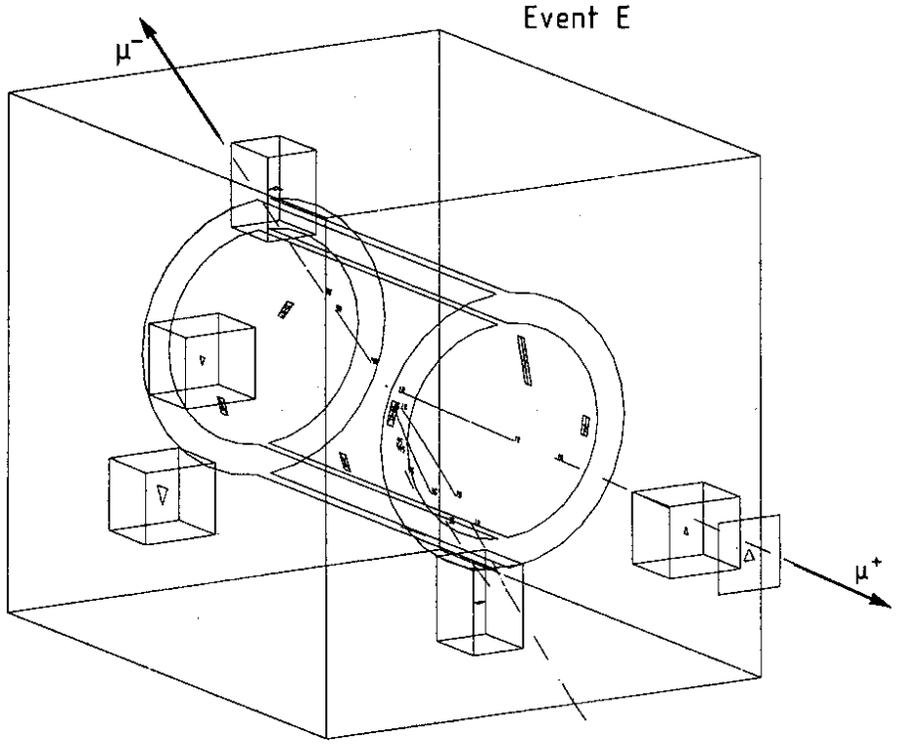

Fig. 5

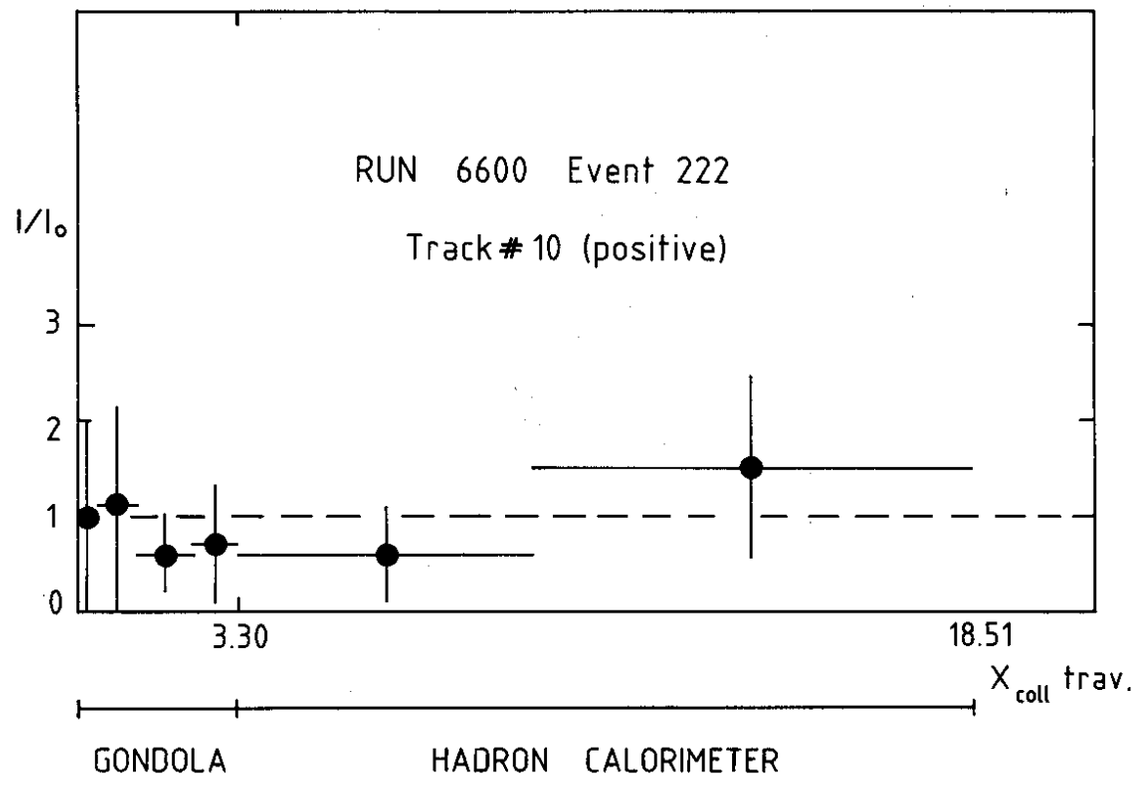
RUN 6600 Event 222
Track # 10 (positive)
I/I₀
3
2
1
0
3.30
18.51
X coll trav.
GONDOLA
HADRON CALORIMETER

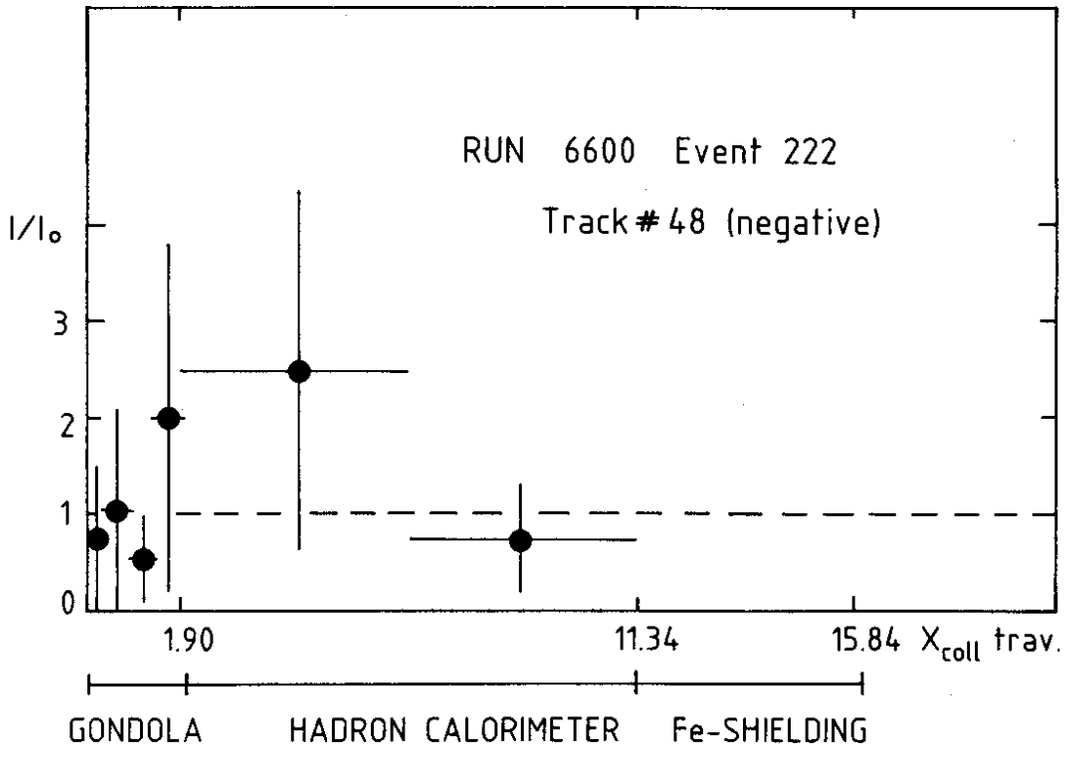
RUN 6600 Event 222
Track # 48 (negative)
I/I₀
3
2
1
0
1.90
11.34
15.84 X coll trav.
GONDOLA
HADRON CALORIMETER
Fe-SHIELDING

Fig. 6a

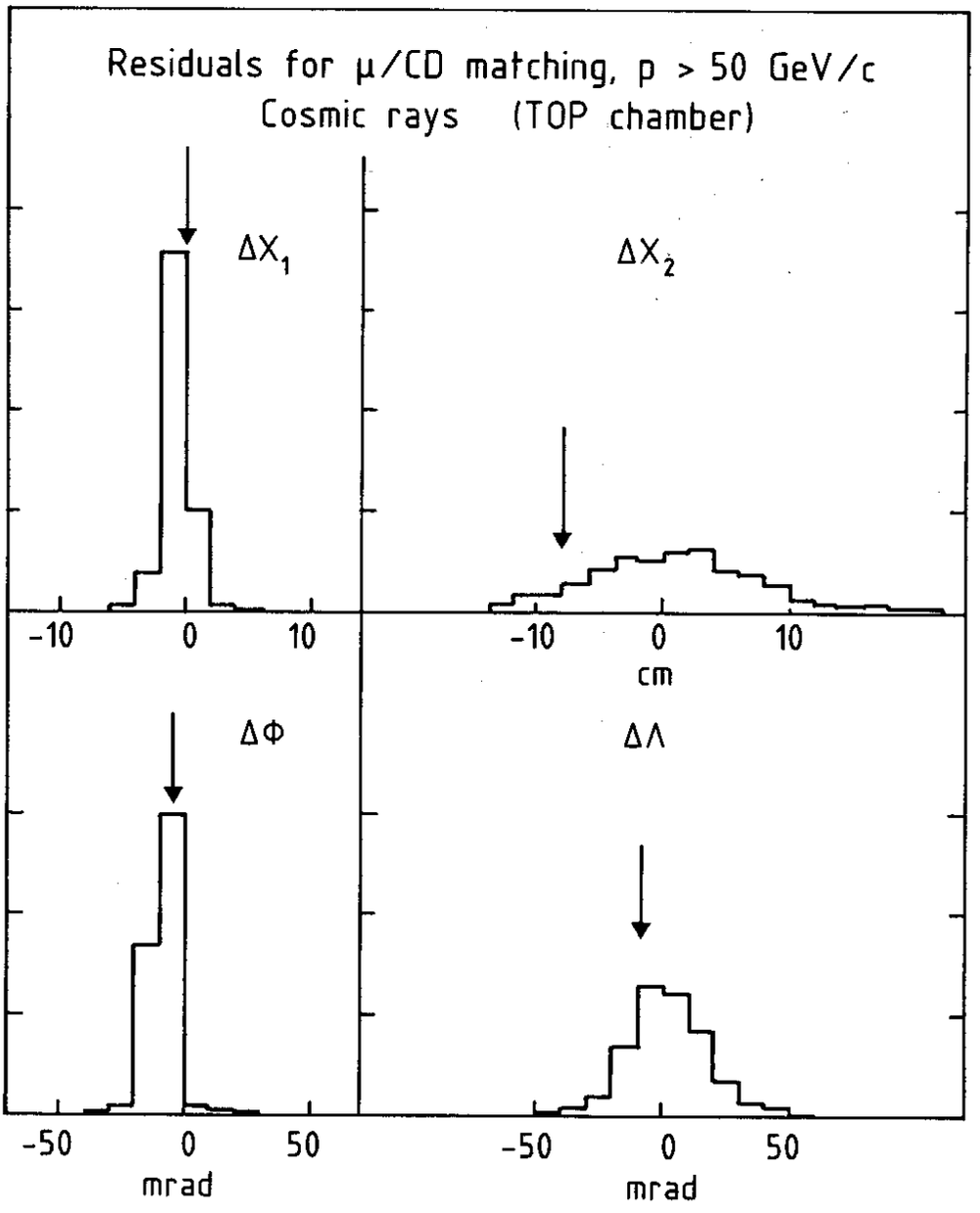
Residuals for μ/CD matching, p > 50 GeV/c
Cosmic rays (TOP chamber)
ΔX1
ΔX2
-10
0
10
-10
0
10
cm
ΔΦ
ΔΛ
-50
0
50
mrad
-50
0
50
mrad

Fig. 6b

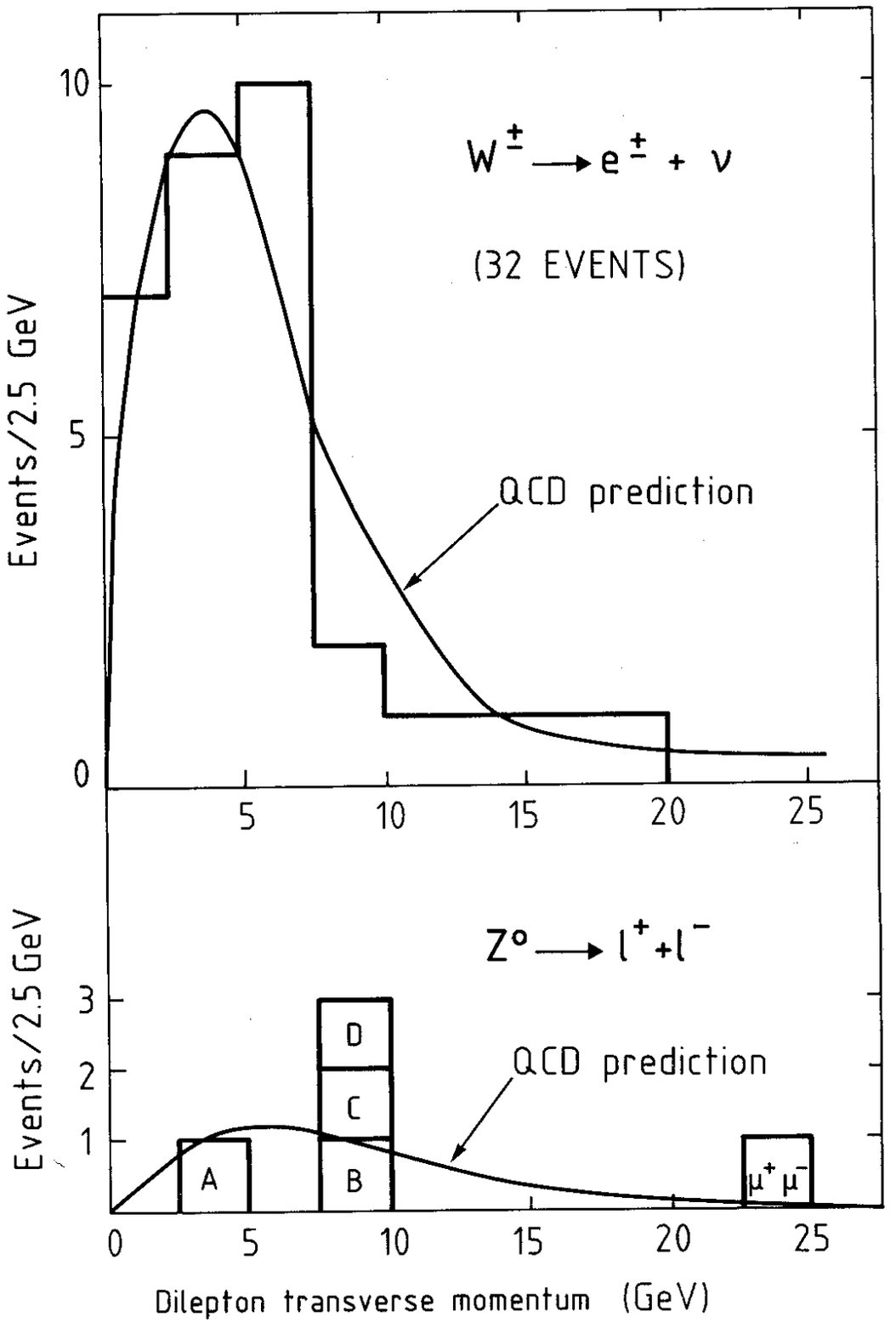
10
5
0
Events/2.5 GeV
$W^{\pm} \longrightarrow e^{\pm} + \nu$
(32 EVENTS)
QCD prediction
5
10
15
20
25
$Z^{o} \longrightarrow l^{+}+l^{-}$
3
2
1
Events/2.5 GeV
D
C
B
A
QCD prediction
$\mu^{+}\mu^{-}$
0
5
10
15
20
25
Dilepton transverse momentum (GeV)

Fig. 7

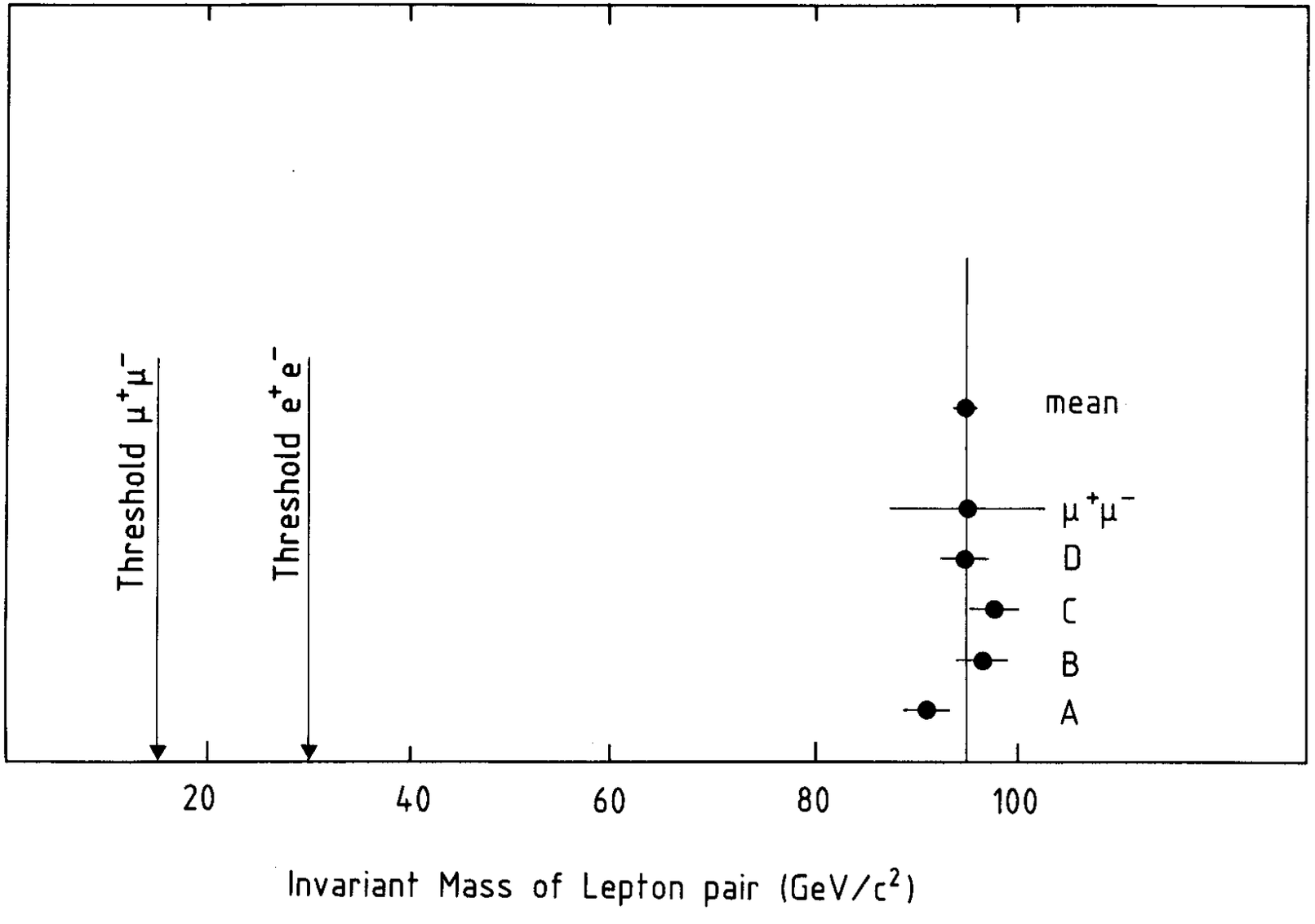
Threshold $\mu^+\mu^-$
Threshold e^+e^-
mean
$\mu^+\mu^-$
D
C
B
A
20
40
60
80
100
Invariant Mass of Lepton pair (GeV/c^2)

Fig. 8

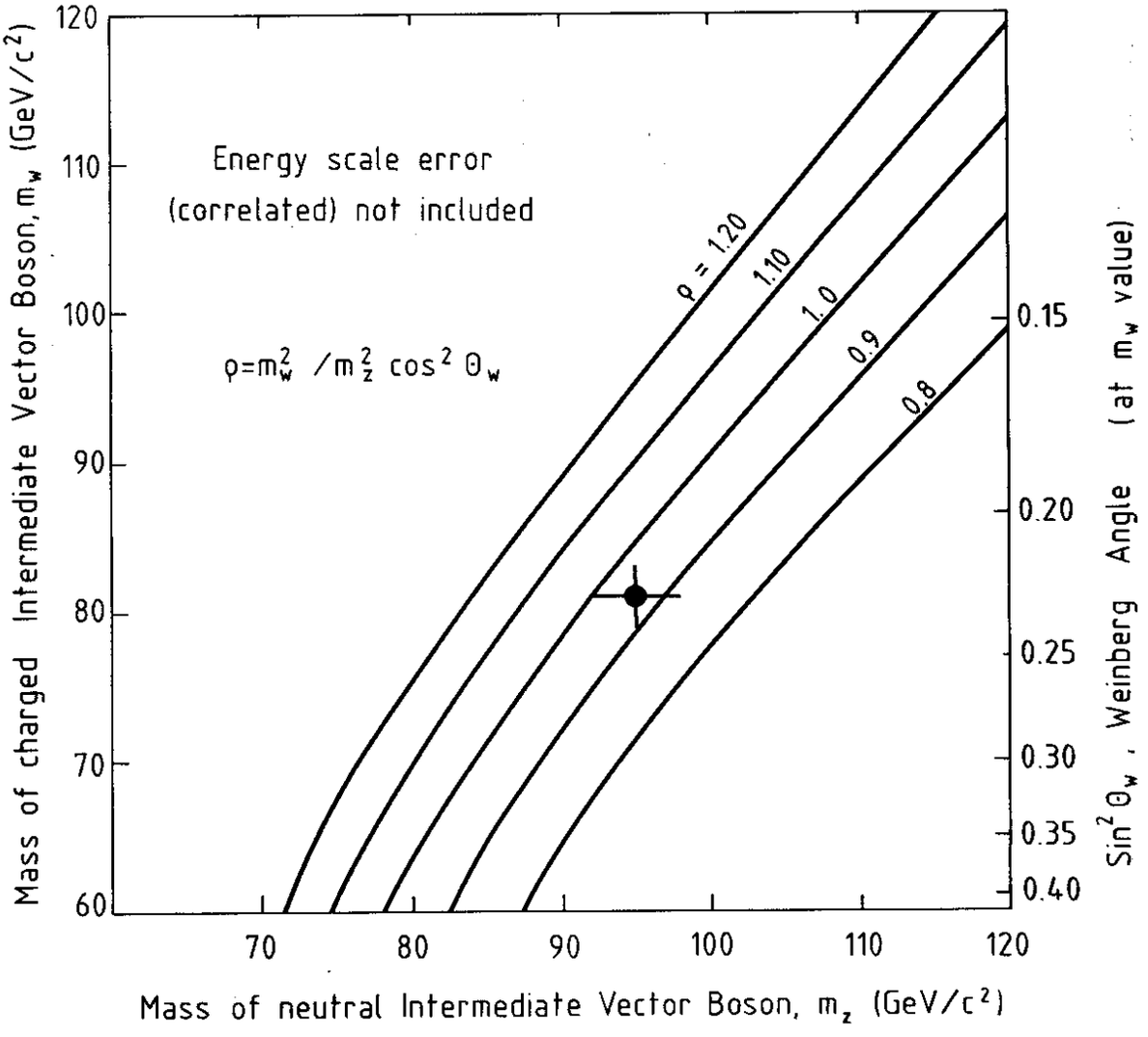
Energy scale error
(correlated) not included
$\rho = m_W^2 / m_Z^2 \cos^2 \theta_W$
$\rho = 1.20$
1.10
1.0
0.9
0.8
Mass of charged Intermediate Vector Boson, m_W (GeV/c^2)
Mass of neutral Intermediate Vector Boson, m_Z (GeV/c^2)
$\sin^2\theta_W$, Weinberg Angle (at m_W value)
120
110
100
90
80
70
60
70
80
90
100
110
120
0.15
0.20
0.25
0.30
0.35
0.40

Fig. 9